

# Analysis of the correlation between horizontal wind and 11-year solar activity over Langfang, China

Bing Cai<sup>1,2</sup>, QingChen Xu<sup>1\*</sup>, Xiong Hu<sup>1</sup>, Xuan Cheng<sup>1</sup>, JunFeng Yang<sup>1</sup>, and Wen Li<sup>1</sup>

<sup>1</sup>Key Laboratory of Science and Technology on Environmental Space Situation Awareness, National Space Science Center, Chinese Academy of Sciences, Beijing 100190, China;

<sup>2</sup>College of Earth Sciences, University of Chinese Academy of Sciences, Beijing 100049, China

## Key Points:

- The responses of atmospheric horizontal wind and tides at the height of 80–100 km to 11-year solar activities are analysed.
- The zonal/meridional wind is positively correlated with solar activities in spring and summer, and the amplitude of annual and semiannual oscillations of the zonal/meridional wind is mainly negatively correlated with solar activities.
- A mechanism is proposed that the solar activities could affect the stratospheric thermal and wind structure, leading to change of upward propagating gravity wave net flux, and finally affect the MLT atmospheric wind field.

**Citation:** Cai, B., Xu, Q. C., Hu, X., Cheng, X., Yang, J. F. and Li, W. (2021). Analysis of the correlation between horizontal wind and 11-year solar activity over Langfang, China. *Earth Planet. Phys.*, 5(3), 270–279. <http://doi.org/10.26464/epp2021029>

**Abstract:** In this study, long term observations of medium frequency (MF) radar at Langfang site (39.4°N, 116.7°E) from 2009 to 2020 have been used to analyze the dependence of the 11-year solar cycle on horizontal winds in the local mesosphere and lower thermosphere (MLT). The results show that the zonal wind is positively correlated with solar activity during spring at 80–84 km, and during summer at 80–82 km; the meridional wind is positively correlated with solar activity during spring at 84–88 km and during summer at 84–90 km. In contrast, the results show no correlation between the horizontal wind and solar activity in autumn and winter. We attempt to explain the correlations in terms of the changes in stratospheric temperature and the net flux of gravity waves during solar activities. In addition, annual and semiannual oscillations of the zonal/meridional wind were found by using the least squares fitting method on daily horizontal winds, which show negative correlations with solar activity at heights of 80–90 km.

**Keywords:** MF radar; MLT; horizontal wind; solar cycle

## 1. Introduction

The response of the 80–100 km mesosphere and lower thermosphere (MLT) winds to the 11-year solar cycle has been intensively studied since the 1960s, and the results have enriched our understanding of MLT dynamic processes. The initial investigation of the solar cycle dependence of winds at 95 km was conducted using night-time wind field data from 1957 to 1965 by Sprenger and Schminder (Sprenger and Schminder, 1968). They found a positive correlation between the prevailing zonal wind and solar activity in winter, with an increase from about 15 m/s during solar minimum to nearly 40 m/s during solar maximum (assuming the westerly and southerly winds are positive). The meridional wind is also positively correlated with solar activity, but with a relatively weak correlation. The semidiurnal tides, both zonal and meridional, are negatively correlated with solar activity. The results were confirmed by Dartt who analyzed composite data from 1966 to 1981 for 90 km (Dartt et al., 1983). Using medium frequency (MF)

radar data from 1979 to 1990, Namboothiri also found a positive correlation between solar activity and the zonal wind in winter and a negative correlation with the meridional wind in summer at heights of 79–97 km, but the confidence level was weak (Namboothiri et al., 1993). He also reported a negative correlation between solar activity and the semidiurnal tide and no obvious correlation with the diurnal tide. All these studies indicated that the horizontal wind is positively correlated with the solar activity in winter, and is negatively correlated with the solar activity in spring and summer, which has been confirmed by Bremer et al. (Bremer et al., 1997; Jacobi, 1998; Keuer et al., 2007).

However, other authors have drawn different conclusions. Using a longer time series of observations at the same site, Gresiger found that during 1957–1984, the zonal wind at 95 km in winter was negatively correlated with solar activity with a correlation coefficient of  $-0.93$  (Gresiger et al., 1987), opposite to Sprenger and Schminder's study. Gresiger also found a negative correlation between the summer zonal wind and solar activity from 1976 to 1983, but no correlation between the meridional wind and solar activity. The negative correlation between the winter zonal wind and solar activity was confirmed by Merzlyakov using wind field data of meteor radar for 90–100 km from 1964 to 1995

Correspondence to: Q. C. Xu, [xqc@nssc.ac.cn](mailto:xqc@nssc.ac.cn)  
Received 25 JAN 2021; Accepted 16 MAR 2021.  
Accepted article online 14 APR 2021.  
©2021 by Earth and Planetary Physics.

(Merzlyakov and Portnyagin, 1999). Middleton analyzed meteor winds for 1988–2000 and found a negative correlation between solar activity and the horizontal wind (Middleton et al., 2002). In addition, he reported a positive correlation between the zonal wind and solar activity in summer and autumn.

Most studies discovered correlations between solar activity and the zonal wind in spring, summer and winter, and correlations between solar activity and the meridional wind in winter. Only a few studies found a positive correlation between the meridional wind and solar activity in spring and summer, e.g., Dartt et al. (Dartt et al., 1983; Merzlyakov and Portnyagin, 1999; Keuer et al., 2007).

As for the correlation between tides and solar activity in the MLT, a negative correlation was found for the semidiurnal tide in summer and winter (Sprenger and Schminder, 1968; Greisiger et al., 1987; Namboothiri et al., 1993; Guharay et al., 2019), except for Keuer who reported no obvious correlation (Keuer et al., 2007). So far, few studies have been conducted on the correlations between diurnal tide and solar activity.

In this study, continuous wind observations of MF radar at Langfang site (39.4°N, 116.7°E) from 2009 to 2020 were used to analyze the dependence of season and solar cycle on the horizontal winds in local MLT, which cover two solar minima and one solar maximum. The correlation of prevailing wind with solar activity was analyzed and the results were compared with other observations.

## 2. Data

MF radar can be used to obtain the atmospheric horizontal wind and electron density at 60–100 km, using full correlation analysis

and differential absorption experiments, respectively. Contributing continuous observations and high time resolution at relatively low cost, there are currently over fifty MF radars all over the world. The National Space Science Center, Chinese Academy of Sciences, has installed an MF radar at Langfang site (39.4°N, 116.7°E) in 2009. This radar has been continuously operated for nearly 12 years with height and time resolutions of 2 km and 4 min, respectively. The main parameters are listed in Table 1, and statistics of these observation are shown in Figure 1. A series of studies have been carried out with these data, such as the seasonal variation of MLT mean wind and tides, the effect of stratospheric sudden warming in mid/low-latitude MLT region, ionospheric D region electron density variations during solar flares, etc. (Yang JF, 2016; Yang JF et al., 2017; Quan L et al., 2021).

Solar activity has a period of about 11 years. The data used in this paper is from 2009 to 2020, corresponding to the 24th cycle of solar activity. This cycle begins at the end of 2009, reaches its peak in 2014 and ends at the beginning of 2020. Years of different solar

**Table 1.** Langfang MF observation parameters.

Parameter	MF radar
Frequency	1.99 MHz
Pulse repetition frequency	80 Hz (daytime); 40 Hz (nighttime)
Height resolution	2 km
Time resolution (the length of individual time series)	4 min
Height	60–110 km
Number of coherent integrations	2

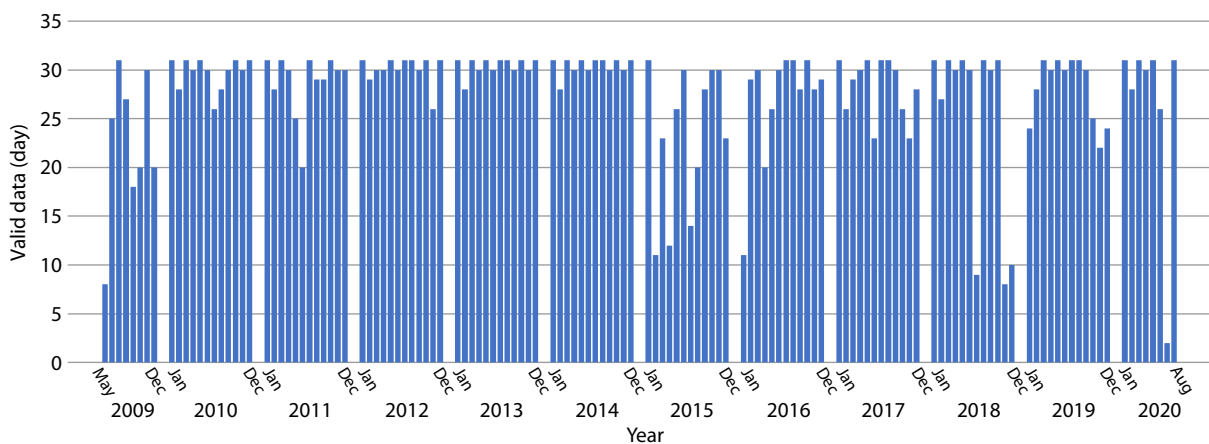


**Figure 1.** Statistics of the observation data.

activity levels can be divided into maximum year and minimum year according to the changes of  $F_{10.7}$ . Figure 2 shows the annual averaged  $F_{10.7}$  from 2009 to 2020. According to the trend of  $F_{10.7}$  in this figure, and excluding the fast-rising and fast-declining years, we consider 2012–2014 as the solar maximum years, and 2009–2010 and 2017–2020 as the solar minimum years. The  $F_{10.7}$  data can be downloaded from the following website: <http://www.spaceweather.gc.ca/solarflux/sx-en.php>.

[spaceweather.gc.ca/solarflux/sx-en.php](http://www.spaceweather.gc.ca/solarflux/sx-en.php).

## 3. Correlation Analysis

The daily zonal and meridional wind at 80–100 km altitude using MF radar were first averaged within a sliding window of 54 days in order to extract the low frequency changes in wind estimation, and filter out high-frequency oscillations such as gravity waves,

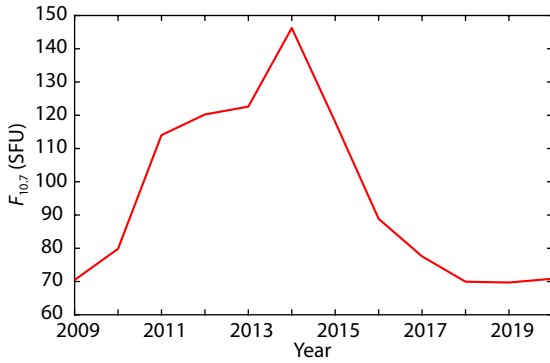


**Figure 2.** The variation of annual averaged  $F_{10.7}$ .

planetary waves, tides, and the 27-day sun rotation period. After this filtering, correlation analysis between  $F_{10.7}$  data and the averaged horizontal wind was conducted.

**3.1 Zonal Wind**

Figure 3 shows the variation of the monthly zonal wind at 80–100 km in 2009–2020. At altitudes of 80–85 km, the zonal wind has a strong annual cycle, easterly in summer (roughly colored in red) and westerly in winter (roughly colored in blue), and shows obvious correlation with the solar activity in summer, i.e., the westerly wind was stronger in solar maximum years than in minimum years. Figure 4 shows the seasonal variations of the zonal wind; the zonal wind is greater in 2015 than in 2010 and 2020, from 80 km to 86 km in spring and summer, which shows a positive correlation with solar activity.

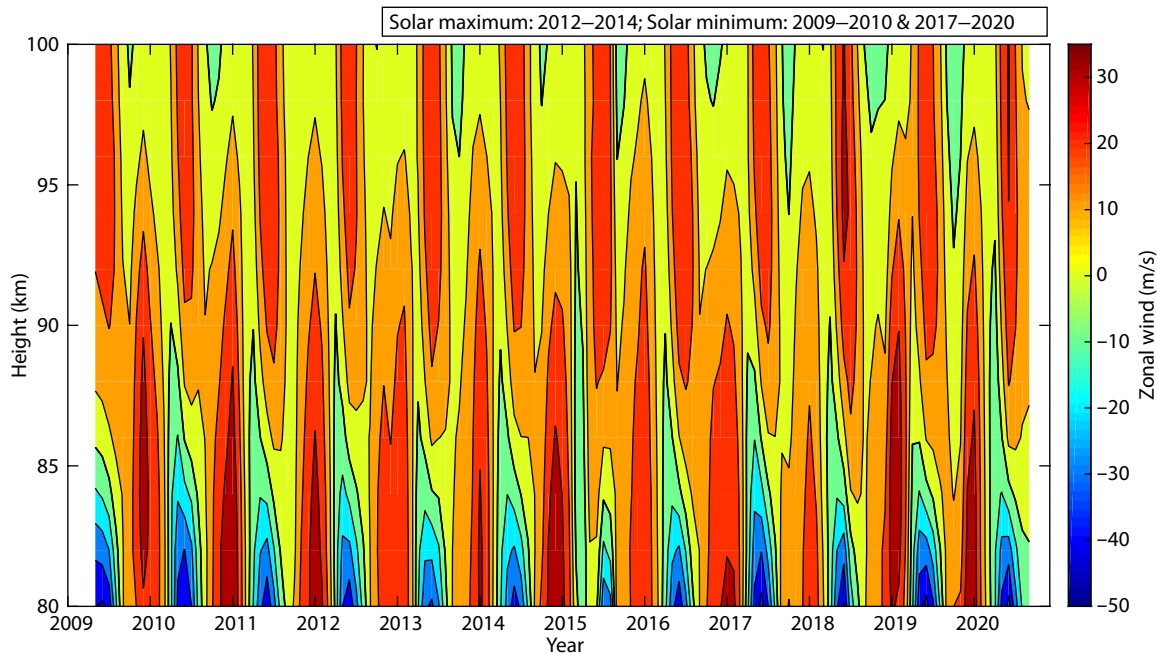
Figure 5 shows the minimum of the 54-day averaged zonal wind and the seasonal averaged  $F_{10.7}$  in spring at 80–84 km, which exhibits a more obvious correlation. In Figure 5, zonal wind is estimated from the three heights to be about  $-15$  m/s in solar maximum

years and  $-40$  m/s in solar minimum years, positively correlated with solar activity. The correlation coefficients for heights of 80, 82, and 84 km are 0.67, 0.66, and 0.55, respectively, and the corresponding confidence levels are better than 98%, 98%, and 93%, which means the higher the altitude, the lower the correlation. The method of calculation of correlation coefficients and confidence levels is similar to Bremer et al. (1997) and Taubenheim (1969). The correlation coefficients from 86 km to 100 km were also calculated, but they are all less than 0.5 and show no significant correlation. Figure 6 is the minimum of the 54-day averaged meridional wind and the seasonal averaged  $F_{10.7}$  in summer at 80–82 km. Zonal wind in summer shows a stronger positive correlation with greater correlation coefficients of 0.81 and 0.65, respectively, and the confidence levels are better than 99% and 98%. However, no correlation was found above 84 km.

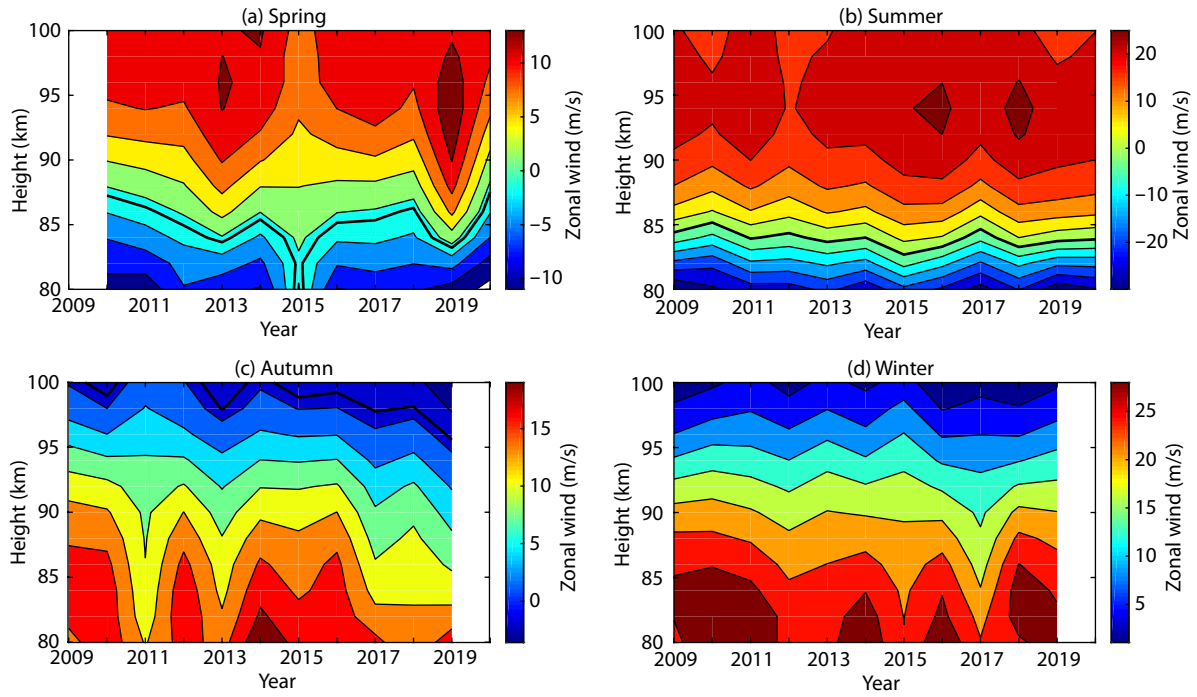
**3.2 Meridional Wind**

Figure 7 shows the variation of the monthly meridional wind at 80–100 km in 2009–2020. It is mainly northerly in summer and southerly in winter at altitudes of 80–90 km, and shows no obvious seasonal changes above 90 km. Since the value of the meridional wind is relatively small, it is difficult to judge its correlation with the 11-year solar activity. Therefore, we studied the seasonal variations of the meridional winds, as shown in Figure 8. There are two minima for the summer meridional wind in 2010 and 2018 at heights of 84–90 km, whereas the value in 2013 is relatively high. This phenomenon exhibits the same trend as solar cycle activity. The correlation analysis was also carried out to the other three seasons, though no similar characteristics were found.

Figure 9 shows the minimum of the 54-day averaged meridional wind and seasonal averaged  $F_{10.7}$  in spring at 84–88 km. In this figure, there are positive correlations with  $F_{10.7}$  at 84, 86, and 88 km, and correlation coefficients are 0.73, 0.64, and 0.57, respectively,



**Figure 3.** Monthly zonal wind at 80–100 km in 2009–2020 (assuming westerly is positive).



**Figure 4.** Seasonal variation of the monthly zonal winds at 80–100 km in 2009–2020: (a) spring: March, April, and May; (b) summer: June, July, and August; (c) autumn: September, October, and November; and (d) winter: December, January, and February.

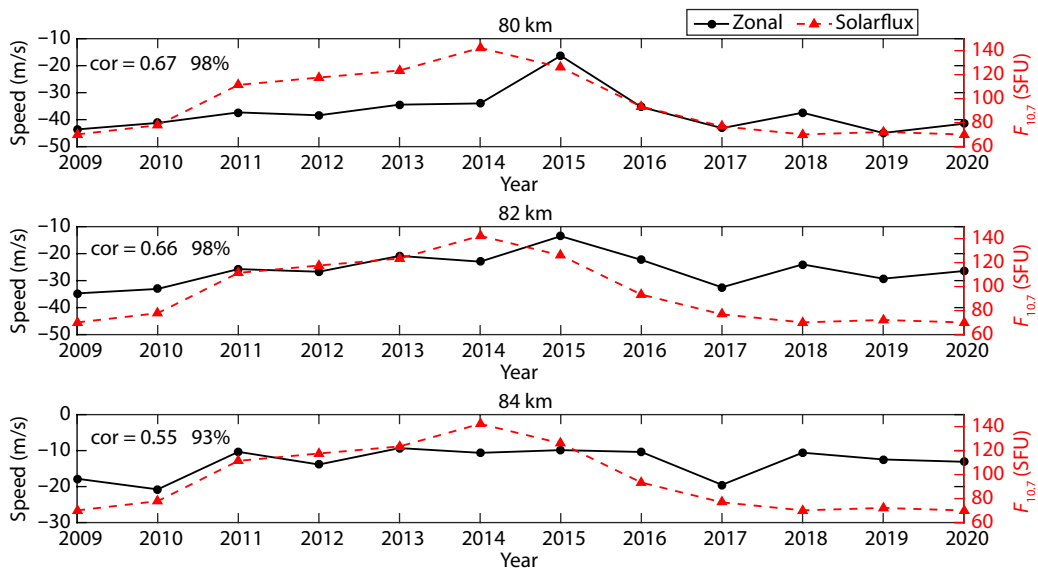


**Figure 5.** Minimum of the 54-day averaged zonal wind and the seasonal averaged  $F_{10.7}$  in spring (80–84 km).

with the confidence levels of better than 99%, 97%, and 94%. **Figure 10** is the minimum of the 54-day averaged meridional wind and seasonal averaged  $F_{10.7}$  in summer from 84 km to 90 km. In **Figure 10**, the meridional wind is about  $-4.7$  m/s in solar maximum years and  $-7$  m/s in solar minimum years, and exhibits an obvious positive correlation with  $F_{10.7}$ . The correlation coefficient is 0.67 with confidence level  $>97\%$ .

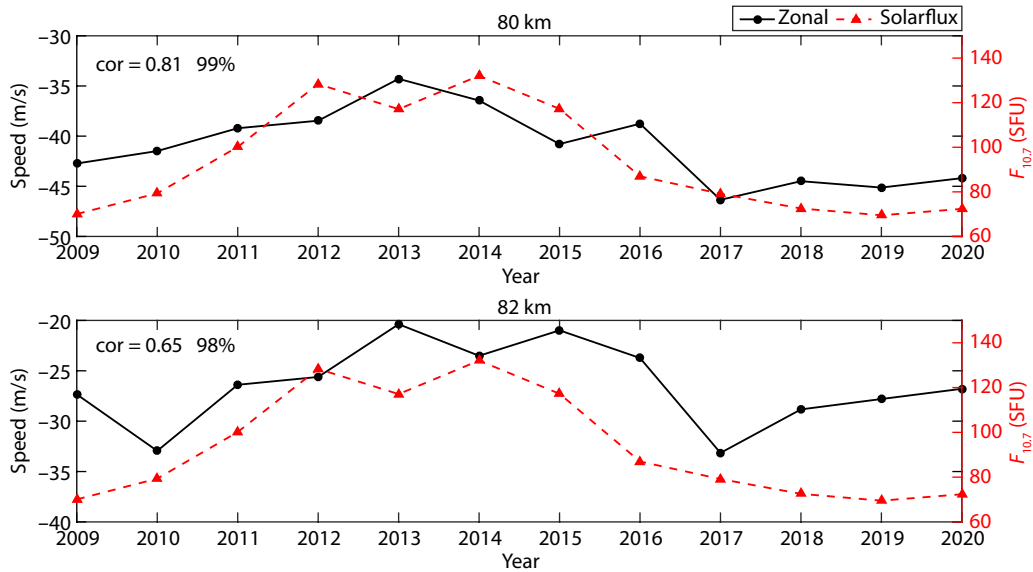
**3.3 Annual and Semiannual Oscillations**

Harmonic analysis was conducted on the daily wind data with a window of three years using the least squares fitting method

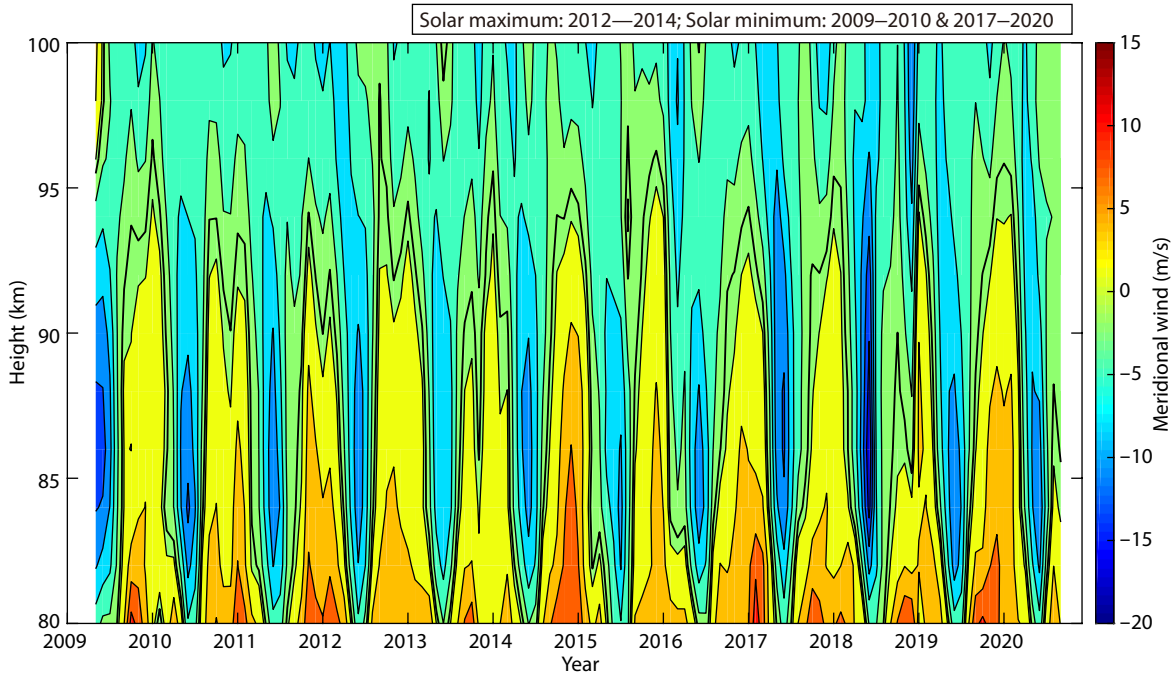
(Equation (1)) to analyze the annual and semiannual oscillations:

$$Y(t) = Y_0 + \sum_{n=1,2} A_n \cos \left[ \frac{2\pi n}{366} (t - \varphi_n) \right], \quad (1)$$

where  $n = 1/2$  is the annual/semiannual oscillation;  $t$  is time;  $Y(t)$  is the daily zonal/meridional wind;  $Y_0$  is the prevailing wind in each window; and  $A$  and  $\varphi$  are the amplitude and phase of the oscillation. The parameters in Equation (1) were only calculated when valid data in each window covered more than 1.5 years. Due to the incomplete data in 2009 and 2020, only the annual and semiannual oscillations from 2010 to 2019 were extracted in this study.



**Figure 6.** Minimum of the 54-day averaged zonal wind and the seasonal averaged  $F_{10.7}$  in summer (80–82 km).



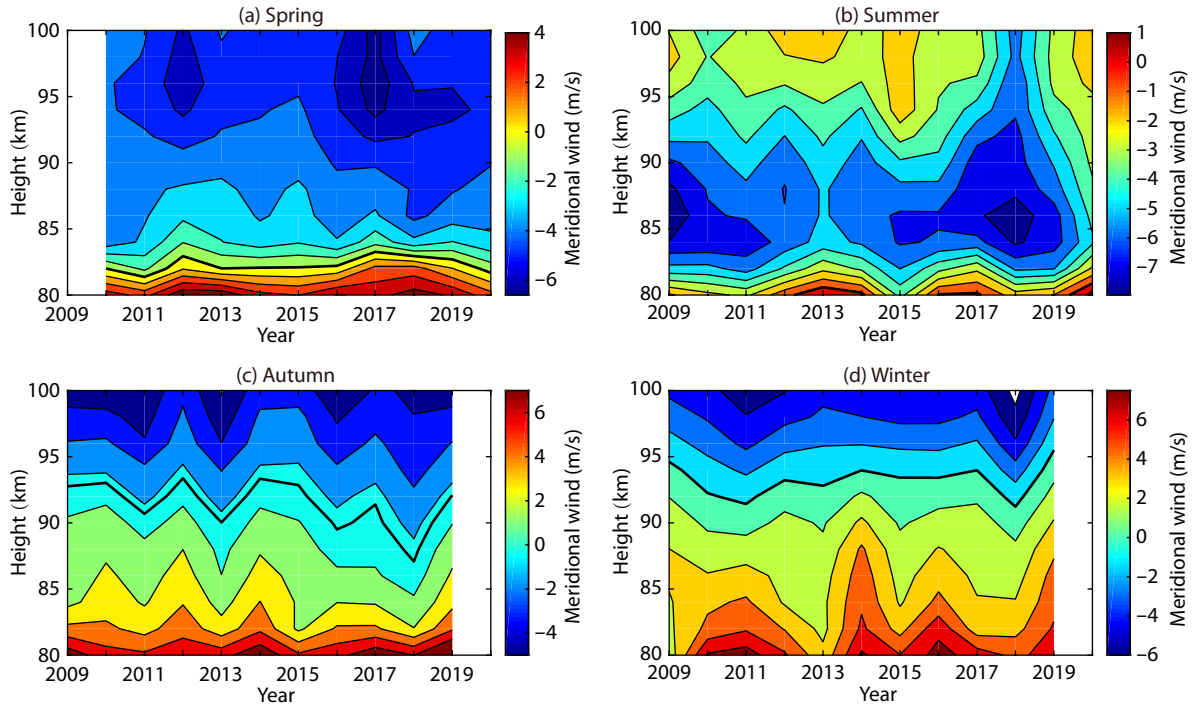
**Figure 7.** Monthly meridional wind at 80–100 km in 2009–2020 (assuming southerly is positive).

Figure 11 shows the amplitudes of the annual and semiannual oscillations of the zonal wind and its correlation coefficients with  $F_{10.7}$  from 80 km to 100 km. It's clear that the annual oscillation of the zonal wind is stronger around 80–85 km and 100 km, while the semiannual oscillation is stronger around 90 km. Furthermore, the annual oscillation and  $F_{10.7}$  are mostly negatively correlated, especially at 92–100 km where the correlation coefficient was about  $-0.75$ . However, MF radar winds are susceptible to interference from factors such as total reflection, the triangle size effect, and receiver saturation in these altitudes (Cervera and Reid, 1995). The results above 90 km were not further studied. The zonal amplitude of the semiannual oscillation is also negatively correlated

with solar activity, and shows an obvious valley at 80–90 km during solar maximum years. The correlation coefficient is about  $-0.7$ , with a confidence  $> 95\%$ . Figure 12 is similar to Figure 11 but for meridional annual and semiannual oscillations. They are mostly negatively correlated with  $F_{10.7}$ , especially at 80 km and 86 km for annual oscillation and at 80–94 km for the semiannual oscillation.

**4. Discussion**

Table 2 summarizes the responses of MLT winds and tides to solar activity since the 1960s. It shows the influence of solar activity on MLT winds is relatively weak, and is easily affected by the observation period, altitude, location, and methods (Bremer et al., 1997). It



**Figure 8.** Seasonal variation of the monthly meridional wind at 80–100 km in 2009–2020: (a) spring: March, April, and May; (b) summer: June, July, and August; (c) autumn: September, October, and November; and (d) winter: December, January, and February.

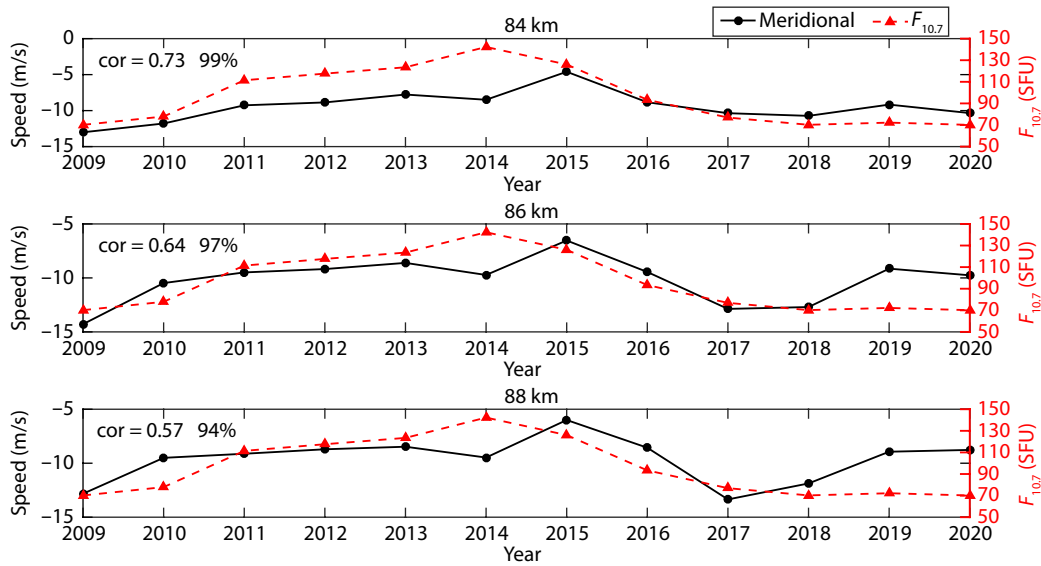


**Figure 9.** Minimum of the 54-day averaged meridional wind and the seasonal averaged  $F_{10.7}$  in spring (84–88 km).

has also been demonstrated that the solar cycle’s effect on mesospheric circulation decreases rapidly above 80 km (Arnold and Robinson, 1998). Therefore, it is understandable that different authors have obtained different results. For example, our analysis of the positive correlations between spring and summer zonal winds and solar activity are consistent with the results of Middleton (Middleton et al., 2002), but are contrary to the results of Dartt et al. (Dartt et al., 1983; Namboothiri et al., 1993; Jacobi, 1998; Keuer et al., 2007). The positive correlations between spring and summer meridional winds and solar activity drawn from our study are

in agreement with the results of Dartt et al. (Dartt et al., 1983; Merzlyakov and Portnyagin, 1999; Keuer et al., 2007), but other studies have reported that there is no obvious correlation (Middleton et al., 2002). There are several possible explanations for these differences, as follows:

- (1) The correlation in the mid-latitudes at 90 to 100 km may be due to an internal atmospheric cause, such as climatic characteristics with a time scale of about 10 years. Therefore, the analysis based on data less than two solar cycles may lead to incorrect results.

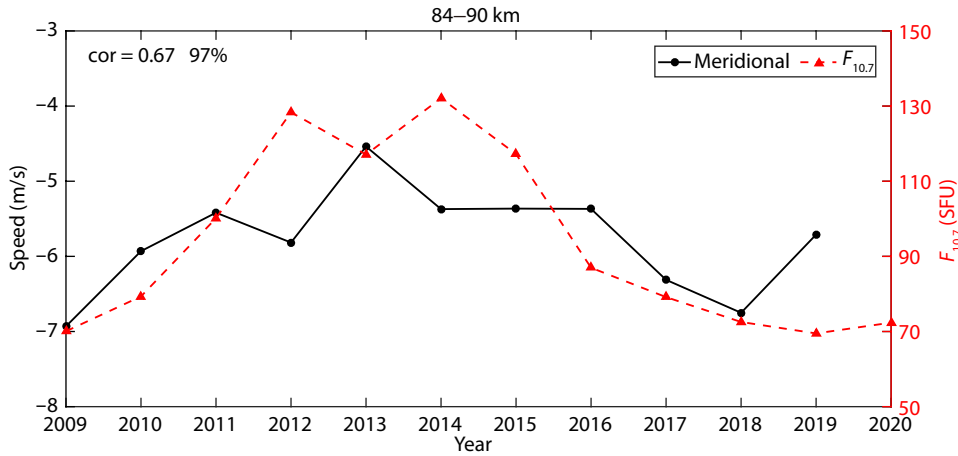


**Figure 10.** Minimum of the 54-day averaged meridional wind and the seasonal averaged  $F_{10.7}$  in summer (84–90 km).

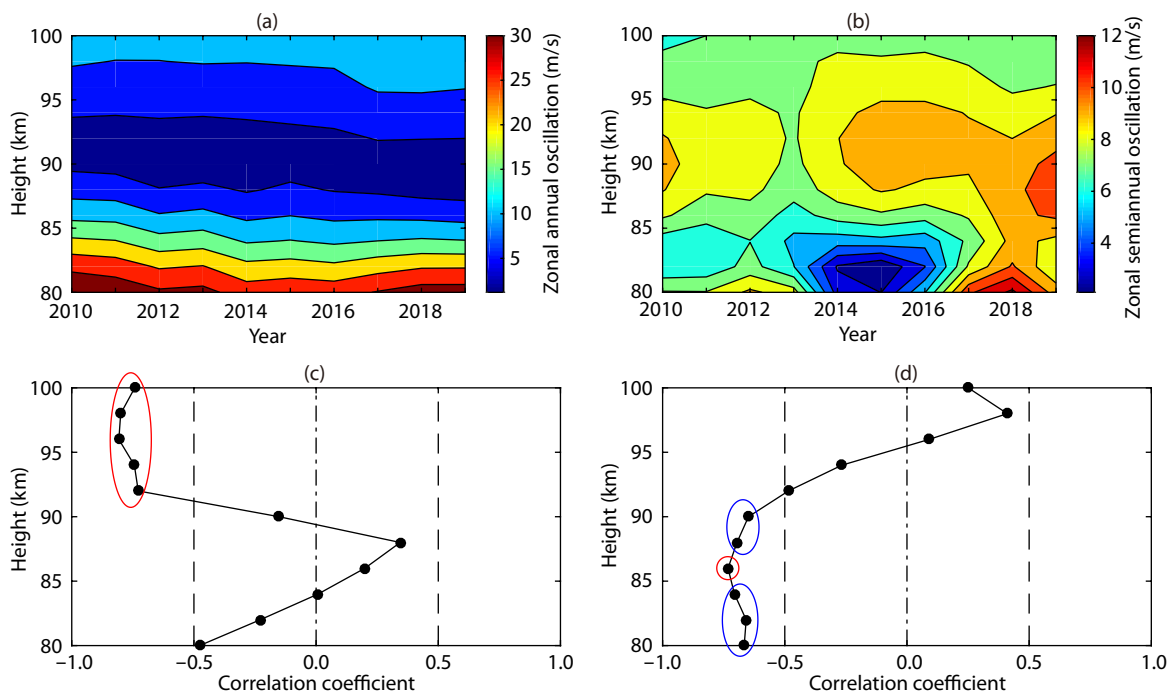


**Figure 11.** (a) variation of the amplitude of the zonal annual oscillation; (b) variation of the amplitude of the zonal semiannual oscillation; (c) correlation coefficients of the amplitude of the zonal annual oscillation with  $F_{10.7}$ ; (d) correlation coefficients of the amplitude of the zonal semiannual oscillation with  $F_{10.7}$  (The circles represent the confidence levels, red: > 98%; blue: > 95%; and green: > 90%).

- (2) The turbulence and momentum deposition generated by breaking gravity waves have an effect on the amplitude and direction of mesospheric circulation.
- (3) Stratosphere and mesosphere temperature changes due to solar activity may indirectly affect the winds in the mesosphere.
- (4) The correlation may be a result of the vertical gradient of the prevailing zonal wind, systematic reflection height changes, and the force exerted by the lower atmosphere.
- (5) Different observing techniques may lead to different responses to solar activity, which varies with height. For example, the best MF radar winds are generally collected below 90 km, while the best meteor radar winds are usually collected at 90–95 km.
- (6) The response of the atmosphere to solar activity may change

from cycle to cycle, thus observations over several decades are required to reveal the true correlations.

In this study, a positive correlation between the 11-year solar cycle and the zonal/meridional prevailing wind in spring and summer was found at heights of 80–90 km, i.e., the westerly/southerly wind was stronger during solar maximum than during solar minimum, whereas no correlation was found in the other seasons and at other heights. According to previous observations, the content of oxygen molecules and ozone is relatively low in the mesopause region (Bowman and Krueger, 1985), and MLT is warm in winter and cool in summer. Thus, the radiation in summer is low during solar activity, which results in small temperature changes, and the effect on the wind is negligible. On the other hand, the

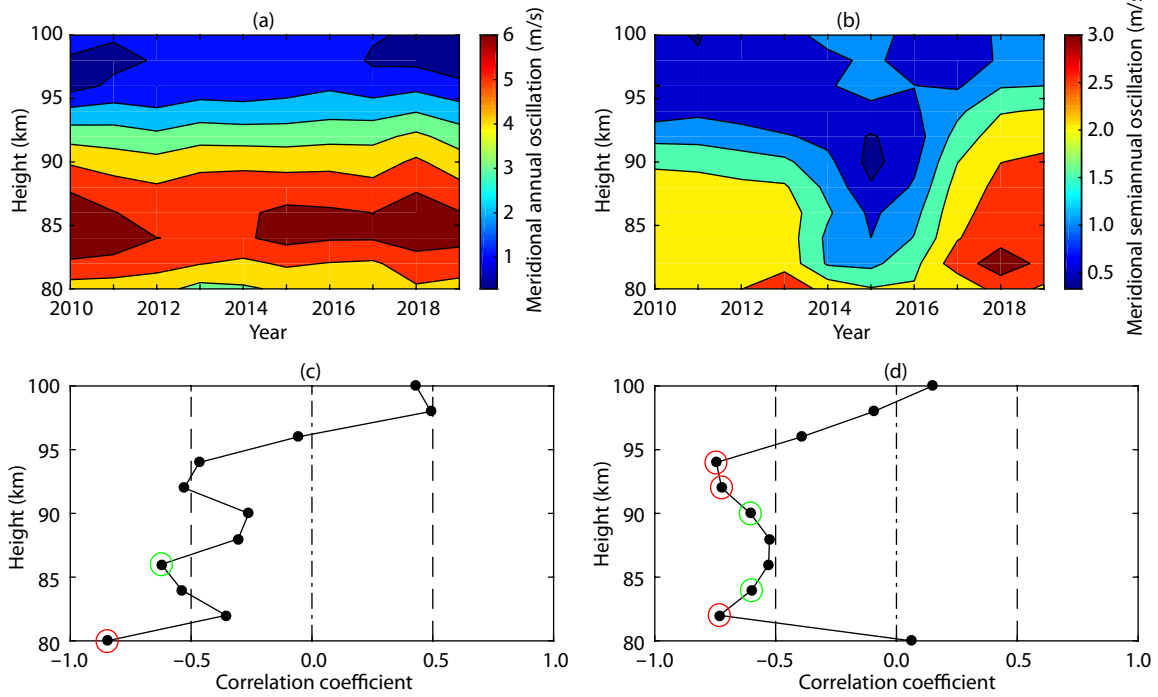


**Figure 12.** (a) variation of the amplitude of the meridional annual oscillation; (b) variation of the amplitude of the meridional semiannual oscillation; (c) correlation coefficients of the amplitude of the meridional annual oscillation with  $F_{10.7}$ ; (d) correlation coefficients of the amplitude of the meridional semiannual oscillation with  $F_{10.7}$  (The circles represent the confidence levels, red: > 98%; blue: > 95%; and green: > 90%.)

**Table 2.** The response of the MLT wind and tides to solar activity since the 1960s (+: positive; -: negative).

Author	Location	Year	Height (km)	Wind	
				Zonal	Meridional
Sprenger and Schminder	Kuhlungsborn (51.4°N, 11.8°E), Collm (51.3°N, 13.0°E)	1957–1968 (nighttime)	95	winter: +	winter: +
Greisiger	Kuhlungsborn (51.4°N, 11.8°E), Collm (51.3°N, 13.0°E)	1975–1984	95	summer: - winter: -	winter: /
Dartt	50°N	1966–1981	90	spring: - summer: - winter: +	spring: + summer: +
			80		
			90 100	same as 50°N	winter: +
Fraser	Adelaide (35°S, 139°E), Christchurch (44°S), Saskatoon (52°N, 107°W), Durham 43°N)	1978–1988	85–95	/	/
Namboothiri	Saskatoon (52°N, 107°W)	1979–1990	79–97	summer: - winter: +	no
Jacobi	Collm (51.3°N, 13.0°E)	1973–1996	95	spring: - summer: -	/
Bremer	Kuhlungsborn (51.4°N, 11.8°E), Collm (51.3°N, 13.0°E)	1964–1994	90–100	summer: - winter: +	winter: + (weak)
Fahrudinova	Kazan State University (46°N, 49°E)	1986–1995	80–110	80–95 km: -	/
Middleton	UK (52°N)	1988–2000	90–95	summer: + autumn: + winter: -	winter: -
Keuer	Juliusruh (54.6°N, 13.4°W)	1990–2005	68–93	summer: - winter: +	summer: + winter: +

drag force of electrons on the horizontal winds may also be negligible due to the relatively low electron density in this region (about 300–400/cm<sup>3</sup>) (Sun W, 2015). So we posit that the response of the horizontal wind at 80–90 km to solar activity is mainly caused by changes in stratosphere temperature and net

momentum of the gravity wave.

According to the thermal wind equation (Equation (2)),

$$f \frac{\partial u}{\partial z} = -\frac{R}{H a} \frac{\partial T}{\partial \phi'} \quad (2)$$

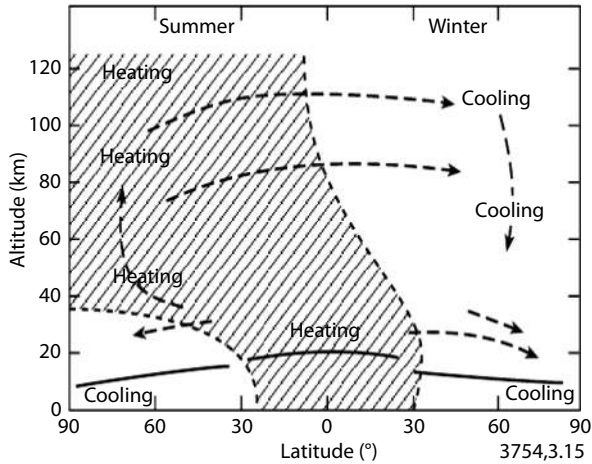


Figure 13. Meridional circulation (Murgatroyd, 1971).

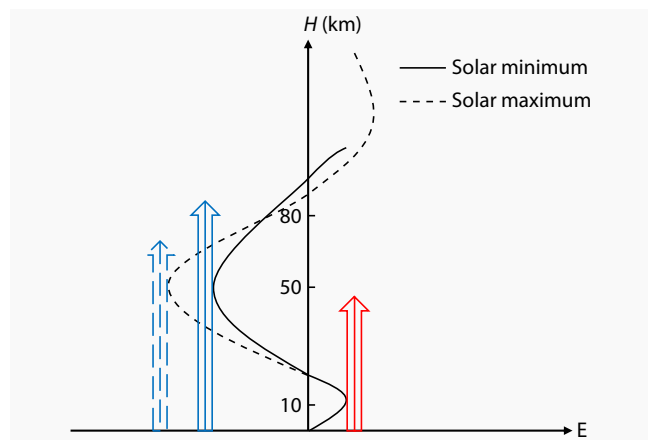


Figure 14. Approximate altitude profiles of the zonal wind in summers during solar maximum years (dashed line) and minimum years (solid line). The arrows indicate upward propagating gravity waves.

where  $f$  is the geostrophic parameter,  $\frac{\partial u}{\partial z}$  is the zonal wind height gradient,  $R$  is the dry air ratio,  $H$  is the geopotential height,  $a$  is the atmospheric density, and the  $\frac{\partial T}{\partial \phi}$  is the temperature meridional gradient, the variation in the zonal wind with height is inversely proportional to the meridional temperature gradient, variation in the zonal wind with height is inversely proportional to the meridional temperature gradient. Figure 13 is a sketch map of the meridional temperature circulation (Murgatroyd, 1971). In this figure, the temperature of the troposphere is higher near the equator than in Langfang (40°N). Thus, the temperature gradient is less than zero, and the zonal wind increases with height. In the stratosphere, the atmospheric temperature increases rapidly with height, because the ozone absorbs the ultraviolet radiation emitted by the Sun, and ozone is more prevalent at mid-latitudes than near the Equator. This leads to the temperature gradient being greater than zero and the zonal wind decreases with height. In the mesosphere, the amplitude of vertical propagating gravity waves increases sharply and generates unstable breaking. The momentum of eastward gravity waves is larger than westward grav-

ity waves, which generates an eastward drag on the zonal wind. Thus the zonal wind increases with height; this variation is shown as the black solid line in Figure 14.

Studies have shown that the stratosphere’s temperature in spring and summer is positively correlated with solar cycle activity, and the correlation is greater at 40°N than near the equator (Gan Q et al., 2016). So in solar maximum years, the temperature gradient (Equation (2)) is greater than in solar minimum years, which results in the zonal wind more rapidly decreasing with height, as is shown by the dashed black line in Figure 14. In addition, the momentum of westward gravity waves decreases due to the larger zonal wind in the stratosphere, while the momentum of eastward gravity waves remains the same, which leads to a larger net eastward momentum and a greater drag on the zonal wind. As the zonal zero wind in summer is above 80 km in Langfang, a positive correlation was found between the solar cycle and the horizontal wind at 80–90 km.

The negative correlation between the solar cycle and the amplitudes of annual oscillations has a close relationship with the positive correlation between the solar cycle and the prevailing wind. As shown in Figure 3, the westerly zonal wind is usually stronger in winter and weaker in the summer. In solar maximum years, the westerly zonal wind is almost constant in winter but increases in summer, which leads to the decreased amplitude of annual oscillations and results in a negative correlation with the solar cycle. Further, a negative correlation between the solar cycle and semi-annual oscillations was found.

### 5. Conclusions

In this study, the Langfang MF radar winds from 2009 to 2020 were used to analyze the responses of the MLT horizontal wind to the 11-year solar cycle activity at different heights and in different seasons. It was found that the zonal wind was positively correlated with solar activity in the spring at 80, 82, and 84 km. The correlation coefficients are 0.67, 0.66, and 0.55 respectively, with confidence levels of greater than 98%, 98%, and 93%, indicating that westerly winds are larger during solar maximum years. A positive correlation was also observed between the summer zonal wind and solar activity at 80 and 82 km, with coefficients of 0.81 and 0.65, respectively, and confidence levels of greater than 99% and 98%. As for the meridional wind, it was positively correlated with solar activity in spring at 84, 86, and 88 km, with the correlation coefficients of 0.73, 0.64, and 0.57, respectively, and confidence levels of greater than 99%, 97%, and 94%, which indicates that the southerly winds are larger during solar maximum years. The summer meridional wind was also positively correlated with solar activity at 84–90 km, with a correlation coefficient of 0.67 and a confidence level > 97%. However, no such correlation was found between autumn and winter horizontal winds and solar activity. Furthermore, annual and semiannual oscillations of the horizontal winds were mainly negatively correlated with the solar cycle.

As for the correlations found in this study, we attempted to explain them in terms of changes in stratosphere temperature and the net momentum of gravity waves in solar maximum years. The regional and time differences of gravity wave activities may be the

main reason for the different conclusions obtained in previous studies. It should be noted that only one solar cycle of horizontal wind data was used in this study. Thus, the conclusions in this paper are only suitable for Langfang at heights of 80–90 km from 2009 to 2020. Surprisingly, we also found seasonal oscillations and even a quasi-biennial oscillation (QBO) in the long-term wind data. Therefore, in future studies, more data will be used to deeply study the mechanisms and processes of horizontal winds, tides, seasonal oscillations, and the QBO dependence on the 11-year solar cycles in Langfang.

### Acknowledgments

This research is supported by the Strategic Priority Research Program of Chinese Academy of Sciences (no. XDA17010302). We acknowledge for the data resources from "National Space Science Data Center, National Science and Technology Infrastructure of China (<https://www.nssdc.ac.cn>)". We would also like to thank the Langfang station for maintaining the MF radar and Space Weather Canada for providing  $F_{10.7}$  data. We thank LetPub ([www.letpub.com](http://www.letpub.com)) for its linguistic assistance during the preparation of this manuscript.

### References

- Arnold, N. F., and Robinson, T. R. (1998). Solar cycle changes to planetary wave propagation and their influence on the middle atmosphere circulation. *Ann. Geophys.*, 16(1), 69–76. <https://doi.org/10.1007/s00585-997-0069-3>
- Bowman, K. P., and Krueger, A. J. (1985). A global climatology of total ozone from the Nimbus 7 total ozone mapping spectrometer. *J. Geophys. Res.*, 90(D5), 7967–7976. <https://doi.org/10.1029/JD090iD05p07967>
- Bremer, J., Schindler, R., Greisiger, K. M., Hoffmann, P., Kürschner, D., and Singer, W. (1997). Solar cycle dependence and long-term trends in the wind field of the mesosphere/lower thermosphere. *J. Atmos. Solar-Terr. Phys.*, 59(5), 497–509. [https://doi.org/10.1016/S1364-6826\(96\)00032-6](https://doi.org/10.1016/S1364-6826(96)00032-6)
- Cervera, M. A., and Reid, I. M. (1995). Comparison of simultaneous wind measurements using colocated VHF meteor radar and MF spaced antenna radar systems. *Radio Sci.*, 30(4), 1245–1261. <https://doi.org/10.1029/95RS00644>
- Dartt, D., Nastrom, G., and Belmont, A. (1983). Seasonal and solar cycle wind variations, 80–100 km. *J. Atmos. Terr. Phys.*, 45(10), 707–718. [https://doi.org/10.1016/S0021-9169\(83\)80029-4](https://doi.org/10.1016/S0021-9169(83)80029-4)
- Gan, Q., Du, J., Fomichev, V. I., Ward, W. E., Beagley, S. R., Zhang, S. D., and Yue, J. (2016). Temperature responses to the 11 year solar cycle in the mesosphere from the 31 year (1979–2010) extended Canadian Middle Atmosphere Model simulations and a comparison with the 14 year (2002–2015) TIMED/SABER observations. *J. Geophys. Res.*, 122(4), 4801–4818. <https://doi.org/10.1002/2016JA023564>
- Greisiger, K. M., Schindler, R., and Kürschner, D. (1987). Long-period variations of wind parameters in the mesopause region and the solar cycle dependence. *J. Atmos. Terr. Phys.*, 49(3), 281–285. [https://doi.org/10.1016/0021-9169\(87\)90063-8](https://doi.org/10.1016/0021-9169(87)90063-8)
- Guharay, A., Batista, P. P., and Andrioli, V. F. (2019). Investigation of solar cycle dependence of the tides in the low latitude MLT using meteor radar observations. *J. Atmos. Solar-Terr. Phys.*, 193, 105083. <https://doi.org/10.1016/j.jastp.2019.105083>
- Jacobi, C. (1998). On the solar cycle dependence of winds and planetary waves as seen from mid-latitude D1 LF mesopause region wind measurements. *Ann. Geophys.*, 16(12), 1534–1543. <https://doi.org/10.1007/s00585-998-1534-3>
- Keuer, D., Hoffmann, P., Singer, W., and Bremer, J. (2007). Long-term variations of the mesospheric wind field at mid-latitudes. *Ann. Geophys.*, 25(8), 1779–1790. <https://doi.org/10.5194/angeo-25-1779-2007>
- Merzlyakov, E. G., and Portnyagin, Y. I. (1999). Long-term changes in the parameters of winds in the midlatitude lower thermosphere (90–100 km). *Izv. Akad. Nauk, Fiz. Atmos. Okeana*, 35(4), 482–493.
- Middleton, H. R., Mitchell, N. J., and Muller, H. G. (2002). Mean winds of the mesosphere and lower thermosphere at 52°N in the period 1988–2000. *Ann. Geophys.*, 20(1), 81–91. <https://doi.org/10.5194/angeo-20-81-2002>
- Murgatroyd, R. J. (1971). Dynamical modelling of the stratosphere and mesosphere. In G. Fiocco (Ed.), *Mesospheric Models and Related Experiments*. Dordrecht: Springer. [https://doi.org/10.1007/978-94-010-3114-1\\_7](https://doi.org/10.1007/978-94-010-3114-1_7)
- Namboothiri S. P., Manson, A. H., and Meek, C. E. (1993). Variations of mean winds and tides in the upper middle atmosphere over a solar cycle, Saskatoon, Canada, 52°N, 107°W. *J. Atmos. Terr. Phys.*, 55(10), 1325–1334. [https://doi.org/10.1016/0021-9169\(93\)90101-4](https://doi.org/10.1016/0021-9169(93)90101-4)
- Quan, L., Cai, B., Hu, X., Xu, Q. C., and Li, L. (2021). Study of ionospheric D region changes during solar flares using MF radar measurements. *Adv. Space Res.*, 67(2), 715–721. <https://doi.org/10.1016/j.asr.2020.10.015>
- Sprenger, K., and Schindler, R. (1968). On the significance of ionospheric drift measurements in the LF range. *J. Atmos. Terr. Phys.*, 30(5), 693–700. [https://doi.org/10.1016/S0021-9169\(68\)80025-X](https://doi.org/10.1016/S0021-9169(68)80025-X)
- Sun, W. (2015). Study on regional ionospheric characteristics based on technique of ground-based GPS and radio occultation (in Chinese). Wuhan: Wuhan University.
- Taubenheim, J. (1969). *Statistische Auswertung Geophysikalischer und Meteorologischer Daten*. Leipzig: Akademische Verlagsgesellschaft Geest & Portig.
- Yang, J. F. (2016). Researches on the variations of atmospheric winds in Near Space at mid-latitude (in Chinese) [Ph. D. thesis]. Beijing: University of Chinese Academy of Sciences.
- Yang, J. F., Xiao, C. Y., Hu, X., and Xu, Q. C. (2017). Responses of zonal wind at ~40°N to stratospheric sudden warming events in the stratosphere, mesosphere and lower thermosphere. *Sci. China Technol. Sci.*, 60(6), 935–945. <https://doi.org/10.1007/s11431-016-0310-8>